

## Kinematics Analysis of In-Parallel 5 DOF Haptic Device

Leng-Feng Lee, Madusudanan S. Narayanan, Frank Mendel, and Venkat N. Krovi  
Department of Mechanical & Aerospace Engineering, University at Buffalo  
and  
Paul Karam, Quanser Inc, Montreal, Canada

### ABSTRACT

Parallel-architecture haptic devices offer significant advantages over serial-architecture counterparts in applications requiring high stiffness and high accuracy. To this end, many haptic devices have been created and deployed by modularly piecing together several serial-chain arms to form an in-parallel system. However, the overall system performance depends both on the nature of the individual arms as well as their interactions. We build on the rich theoretical background of constrained articulated mechanical systems to provide a systematic framework for formulation of system-level kinematic performance from individual-arm characteristics. Specifically, we develop the system-level kinematic model in a symbolic (yet algorithmic) fashion that facilitates: (i) computational development of pertinent symbolic equations; (ii) generalization to arbitrary architectures; and (iii) combined symbolic/numeric analyses of performance (workspace, singularities, design sensitivities). These various aspects are illustrated using the example of the Quanser High Definition Haptic Device (HD)<sup>2</sup> – an in-parallel haptic device formed by coupling two 3-link Phantom 1.5 type serial chain manipulators with appropriate passive joints. We also briefly discuss aspects of ongoing work for design-prototyping and validation, taking advantage of tools from Virtual Prototyping and Hardware-in-the-Loop testing.

**KEYWORDS:** Modeling, Kinematics, Haptic device.

### INDEX TERMS:

### 1 INTRODUCTION

Parallel architecture manipulators consist of a moving platform that is attached to a fixed base by several articulated kinematic chains, creating one or more closed kinematic loops within the system [1-2]. Such parallel-architecture systems are well-known for their low inertia, high rigidity and accuracy, high payload capacity and large bandwidth force-transmission, making them well-suited for force-reflecting hand controllers [3-4].

Recently, there has been considerable interest in *creating parallel-architecture haptic devices as in-parallel systems by a modular composition approach*, wherein multiple articulated serial-chain arms cooperate to control a common end-effector. Such a composite-system can now potentially allow for increased redundancy, robustness, and reliability and even active reconfigurability for different tasks. Further, in promoting reuse of components, such a modular “building-block” approach is also a favorable engineering practice.

However, such modularity *creates increased design-choices*, in terms of methods to realize given tasks, and *requires a design-selection process* to determine the best designs. However, the system performance in a modularly composed system depends both the nature of the individual modules as well as their interactions, which creates challenges. Hence, a systematic (and

preferably computational) framework for evaluation of the design-choices on individual module- and system-level characteristics is desirable.

This is an aspect that we examine in the context of the Quanser High Definition Haptic Device (HD)<sup>2</sup> – an in-parallel haptic device formed by coupling two 3-link Phantom 1.5 type serial chain manipulators to a common end-effector handle. However, the two three-link manipulators cannot be arbitrarily coupled to the handle due to the potential kinematic incompatibility (of the velocities at the end effector). Hence, further passive articulations are necessary in order to accommodate the rigid body constraints. In (HD)<sup>2</sup> system, this role is played by the passive revolute and universal joints.

In general, a careful selection of the type, number, dimensions and actuation of all the joints are critical to determining the performance of the overall system (in terms of workspace, mobility and force transmission capabilities). To this end, we leverage the rich theoretical analysis background for constrained articulated mechanical systems. In particular, we exploit a twist-based analysis of in-parallel systems [5] to create the underlying performance-characterization framework. The novel contributions of this paper come from: (i) algorithmic modeling of the individual arms, especially exploiting symbolic computational tools; (ii) systematic system-level motion analysis, by composing contributions from the individual modules; and (iii) validation within a combined simulation and hardware-in-the-loop environment.

The rest of the paper is organized as follows: Section 2 presents a brief overview of the pertinent literature. Twist based modeling is developed in Section 3. Section 4, analyzes the in-parallel (HD)<sup>2</sup> system in detail. In Section 5, kinematic motion analyses of our system are presented as well as the simulation results. Section 6 concludes the paper with brief discussions.

### 2 BACKGROUND

Although known for a century, in-parallel/cooperating robotic and haptic device architectures have seen significantly increased use only in the past two decades.

From a design-perspective, the physical layout of the parallel haptic device, in terms of selection of the type and number of the in-parallel articulated chains, and their attachment to the mobile platform determines the topology of the system. The subsequent selection of type, number, location and actuation of the individual articulations (within each serial chain) completes the determination of the workspace, mobility, controllability, and overall performance of the system. Various performance measures derived from the generalized Jacobian matrix [6-7] have been employed for design and optimization of such parallel architecture systems.

Systems with closed-kinematic loops have also been studied extensively from both simulation [8-9] as well as control for load distribution [10-12]. The structural stabilization from the closed-kinematic loops is the root cause of the high rigidity and payload capacity. However, such loops also *restrict the overall workspace*,

introduce significant nonlinearities in the analysis and restrict the selection (and coordination) of the actuation within the articulated structure. The difficulties in analytical computation of the direct kinematics for higher degree of freedom (d.o.f) parallel manipulators hampered the development of model-based control methods [13-15]. The presence of closed kinematic chains reduces the effective system degrees of freedom, creating kinematic redundancy and most often redundancy in actuation [16]. A careful resolution of this redundancy is critical to achieving control of such systems for desired motion- and force-exertion tasks, as we will see later in this paper.

### 3 MATHEMATICS BACKGROUND

We briefly summarize the spatial twist-based modeling of the articulated mechanical systems here. An interested reader may refer to Hunt [17] for the more traditional line-based screw-theoretic modeling.

The adopted twist- modeling approach emphasizes the linkage to matrix-Lie group based modeling and analysis of rigid-body mechanics. Specifically, the 3-step process discussed below emphasizes: (i) systematically constructing the twist matrix for each joint in the local proximal frame, from a homogeneous transformation-matrix representation; (ii) transforming the joint twist-matrices into a common reference frame, using adjoint transformations; and (iii) extracting twist vectors and composing into a Twist-Assembled Jacobian Matrix (TAJM).

The relative configuration of a moving frame  $\{E\}$  relative to a fixed frame  $\{F\}$  is defined by the homogeneous transformation expressed in a  $4 \times 4$  matrix form as

$${}^F A_E = \begin{bmatrix} {}^F R_E & {}^F d \\ 0^T & 1 \end{bmatrix} \quad {}^F A_E \in SE(3) \quad (1)$$

where  ${}^F R_E \in SO(3) = \{R \in \mathbb{R}^{3 \times 3} : RR^T = I, \det R = +1\}$  is a rotation matrix, and  ${}^F d \in \mathbb{R}^3$  is a displacement vector. A twist matrix  $T \in se(3)$  can be represented by a  $4 \times 4$  matrix of the form

$$T = \begin{bmatrix} \Omega & v \\ 0^T & 0 \end{bmatrix}, \Omega = \begin{bmatrix} 0 & -\omega_z & \omega_y \\ \omega_z & 0 & -\omega_x \\ -\omega_y & \omega_x & 0 \end{bmatrix} \in so(3) \quad (2)$$

where  $\Omega$  is a skew-symmetric matrix,  $\omega \in \mathbb{R}^3$ , and  $v \in \mathbb{R}^3$ . The twist vector then takes the form of  $\underline{t} = [\omega^T \ v^T]^T \in \mathbb{R}^6$  where  $\omega$  is the angular velocity and  $v$  is a linear velocity vector. An unskew operation may also be defined on the set of twist matrices that allows the extraction of twist vectors as:

$$Unskew(T) = [\underline{t}]^T = [\omega^T \ v^T]^T \quad (3)$$

In general, a *spatial twist matrix* corresponding to the motion of the moving frame  $\{E\}$  with respect to its immediately preceding frame  $\{F\}$  (as expressed in the frame  $\{F\}$ ) can be formed as

$${}^F [{}^F T_E] = [{}^F \dot{A}_E] [{}^F A_E^{-1}] \quad (4)$$

Such a the twist matrix can then be transformed to any arbitrary frame  $\{N\}$  by a similarity transformation as

$${}^N [{}^F T_E] = [{}^N A_F] {}^F [{}^F T_E] [{}^N A_F^{-1}] \quad (5)$$

The forward kinematics of an articulated system with N joints can be formulated in terms of homogeneous transforms as:

$${}^0 A_N = {}^0 A_1 {}^1 A_2 \cdots {}^{N-1} A_N \quad (6)$$

The total twist can be considered as a linear combination of various twist contributions of individual articulated degrees of freedom expressed in a common frame:

$${}^0 [{}^0 T_N] = \underbrace{{}^0 [{}^0 T_1]}_{\bar{T}_1} + \underbrace{{}^0 A_1 [{}^1 T_2] [{}^2 A_1]^{-1}}_{\bar{T}_2} + \underbrace{{}^0 A_2 [{}^2 T_3] [{}^3 A_2]^{-1}}_{\bar{T}_3} + \cdots + \underbrace{{}^0 A_{N-1} [{}^{N-1} T_N] [{}^N A_{N-1}]^{-1}}_{\bar{T}_N} \quad (7)$$

Using Eq. (5), this can be transformed to inertial frame  $\{W\}$  as:

$$\begin{aligned} {}^W [{}^0 T_N] &= [{}^W A_0] {}^0 [{}^0 T_1] [{}^W A_0]^{-1} \\ &= [{}^W A_0] \bar{T}_1 [{}^W A_0]^{-1} + [{}^W A_0] \bar{T}_2 [{}^W A_0]^{-1} + \cdots + [{}^W A_0] \bar{T}_N [{}^W A_0]^{-1} \\ &= \bar{T}_1 + \bar{T}_2 + \cdots + \bar{T}_N \end{aligned} \quad (8)$$

Finally, these twist matrices can be rewritten as linear combinations of twist vectors parameterized by the corresponding manipulation variable rates  $\dot{\eta} = [\dot{\eta}_1 \ \dot{\eta}_2 \ \cdots \ \dot{\eta}_N]^T$ . A twist-assembled Jacobian matrix ( $J_T$ ) may now be constructed in the form of

$${}^W [t] = \underbrace{\begin{bmatrix} \bar{t}_1 & \bar{t}_2 & \cdots & \bar{t}_N \end{bmatrix}}_{J_T} \begin{bmatrix} \dot{\eta}_1 \\ \dot{\eta}_2 \\ \vdots \\ \dot{\eta}_N \end{bmatrix} \quad (9)$$

where  $\bar{t}_i = Unskew(\bar{T}_i)$  are the twist vectors corresponding to the manipulation variable rates of  $\dot{\eta}_1, \dot{\eta}_2, \dots, \dot{\eta}_N$ , respectively. The Jacobian matrix ( $J_T$ ) can be interpreted as the linear operator that maps the contribution of the manipulation variable rate at each actuated joint in the system to the inertial twist at frame  $\{W\}$ .

### 4 HIGH DEFINITION HAPTIC DEVICE

The Quanser High Definition Haptic Device (HD<sup>2</sup>) can be viewed as an in-parallel manipulator created by coupling the end-effectors of two Sensable PHANToM Premium 1.5 devices placed side-by-side to a common handle through a set of universal and revolute joints. The (HD)<sup>2</sup> can now provide controlled motion- and force-feedback along 5 degrees-of-freedom (d.o.f) compared to 3 d.o.f. force-feedback provided by the original Sensable PHANToM Premium 1.5 device. The uncontrolled degree-of-freedom is the rotational direction of the common handle about the axis along its length (i.e.  $z_0$  direction in Figure 2).

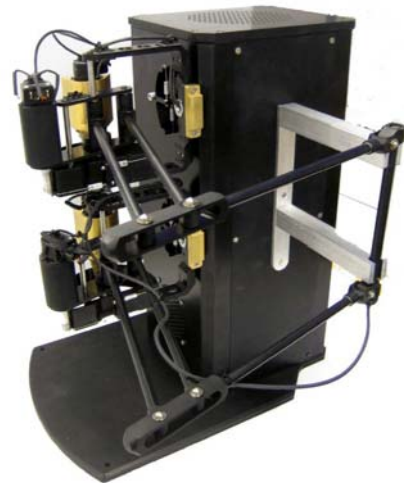


Figure 1. Actual HD<sup>2</sup> system.

#### 4.1 Forward Kinematics

We assign rigid-body frames for each link following the convention for modified DH parameters. As shown in Figure 2, these frames were assigned as  $\{0\}, \{1\}, \dots, \{6\}$ , from the base of the upper chain to the mid-point of the handle. For clarity, we only show the frame assignment for the links of the upper chain and describe the formulation process. A similar process was followed for frame assignment on the lower chain as  $\{0'\}, \{1'\}, \dots, \{6'\}$ . We then develop the table of DH parameters (as shown in Table 1) which facilitates creation of the relative homogeneous transforms between the various frames in a systematic manner.

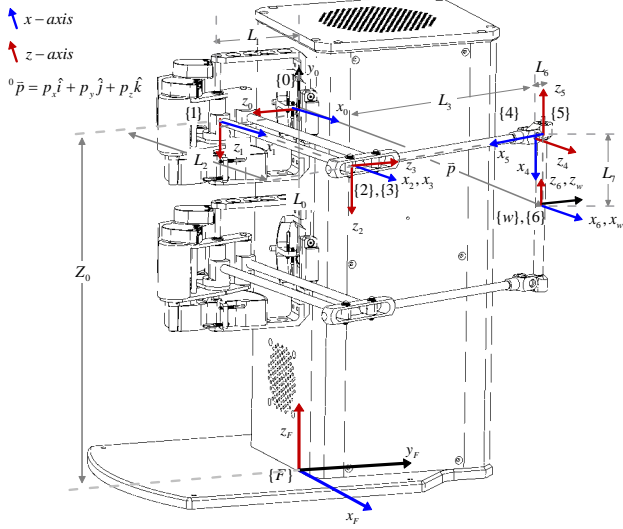


Figure 2. The HD<sup>2</sup> Haptic device and DH frames assignment on the upper arm.

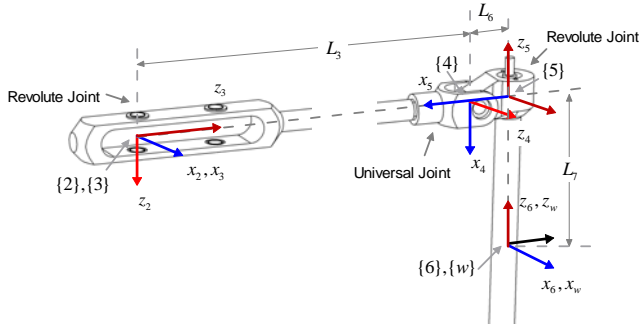


Figure 3. Passive attachment (via universal joint and revolute joint) of the serial-chain's end-effector to the common handle.

$i$	$\alpha_i$	$a_i$	$d_i$	$\theta_i$	$\theta_{i,ini}$
1	$\pi/2$	0	$L_1$	$\theta_1$	0
2	0	$L_2$	0	$\theta_2$	0
3	$\pi/2$	0	0	$\theta_3$	0
4	$\pi/2$	0	$L_3$	$\theta_4$	$\pi/2$
5	$\pi/2$	$-L_6$	0	$\theta_5$	$-\pi/2$
6	0	0	$-L_7$	$\theta_6$	0

Note:  $\theta_1, \theta_2, \theta_3$  – Active joints;  $\theta_4, \theta_5, \theta_6$  – Passive joints.

Table 1. Geometric parameters for the HD<sup>2</sup>.

The benefit of using these DH parameters is it provides the ability to create the relative homogeneous transforms between the

various frames in a systematic manner. The forward kinematics for the overall system can be written as:

$${}^0A_7 = {}^0A_1 {}^1A_2 \dots {}^6A_7 = \begin{bmatrix} {}^0R_7 & {}^0P_7 \\ 0 & 1 \end{bmatrix} \quad (10)$$

We also choose to place an inertial frame  $\{W\}$ , instantaneously coincident with the end-effector frame  $\{6\}$  and the homogenous transformation with respect to the  $\{0\}$  frame can be expressed as:

$${}^wA_0 = \begin{bmatrix} I & -{}^0P_6 \\ 0 & 1 \end{bmatrix} \quad (11)$$

The forward differential kinematic model of such constrained system can generally be written as

$$J_T(\eta) \dot{\eta} = {}^E t \quad (12)$$

with general constraint equations of

$$J_C(\eta) \dot{\eta} = 0 \quad (13)$$

The Jacobian of the upper arm (A) may now be developed as:

$$\begin{bmatrix} \omega \\ v \end{bmatrix} = \begin{bmatrix} | & | & | & | & | & | \\ \$1^A & \$2^A & \$3^A & \$4^A & \$5^A & \$6^A \\ | & | & | & | & | & | \end{bmatrix} \begin{bmatrix} \dot{\theta}_a^A \\ \dot{\theta}_p^A \end{bmatrix} = [J_a^A \quad J_p^A] \begin{bmatrix} \dot{\theta}_a^A \\ \dot{\theta}_p^A \end{bmatrix} \quad (14)$$

where  $[\omega, v]^T = [\omega_x, \omega_y, \omega_z, v_x, v_y, v_z]^T$ ,  $\dot{\theta}_a^A = [\dot{\theta}_1, \dot{\theta}_2, \dot{\theta}_3]^T$  are the active joints,  $\dot{\theta}_p^A = [\dot{\theta}_4, \dot{\theta}_5, \dot{\theta}_6]^T$  are the passive joints,  $J^A = [J_a^A \quad J_p^A]$  is the Jacobian matrix, and  $[\$1, \$2, \dots, \$6]$  are twist vectors. Similarly, the spatial twist  ${}^0[{}^0T_7]$  of the lower link can be expressed as:

$$\begin{bmatrix} \omega \\ v \end{bmatrix} = \begin{bmatrix} | & | & | & | & | & | \\ \$1^B & \$2^B & \$3^B & \$4^B & \$5^B & \$6^B \\ | & | & | & | & | & | \end{bmatrix} \begin{bmatrix} \dot{\theta}_a^B \\ \dot{\theta}_p^B \end{bmatrix} = [J_a^B \quad J_p^B] \begin{bmatrix} \dot{\theta}_a^B \\ \dot{\theta}_p^B \end{bmatrix} \quad (15)$$

Since both Eq. (14) and Eq. (15) are expressions for the same end-effector twist, equating them allows us to express the velocity level constraints as:

$$J_a^A \dot{\theta}_a^A + J_p^A \dot{\theta}_p^A = J_a^B \dot{\theta}_a^B + J_p^B \dot{\theta}_p^B \quad (16)$$

Note that the ability to obtain Eq. (14) and Eq. (15) symbolically allows us to easily identify dependencies (such as the fact that  $\$6^B = \$6^A$ ). Therefore we choose to eliminate  $\$6^B$  and  $\dot{\theta}_6^B$  from Eq. (15), resulting in reduced matrix and vector

$$\tilde{J}^B = \begin{bmatrix} | & | \\ \$4^B & \$5^B \\ | & | \end{bmatrix} \text{ and } \tilde{\theta}_p^B = [\dot{\theta}_4, \dot{\theta}_5]^T \quad (17)$$

The passive joint rates may be expressed in terms of the active joint rate as:

$$\begin{bmatrix} \dot{\theta}_p^A \\ \dot{\theta}_p^B \end{bmatrix} = \underbrace{[-J_p^A \quad J_p^B]^{-1}}_S [J_a^A \quad -J_a^B] \begin{bmatrix} \dot{\theta}_a^A \\ \dot{\theta}_a^B \end{bmatrix} = S \begin{bmatrix} \dot{\theta}_a^A \\ \dot{\theta}_a^B \end{bmatrix} \quad (18)$$

and only  $S_{(4;5,:)}$  is being used.

$$\begin{bmatrix} \dot{\theta}_1^A \\ \vdots \\ \dot{\theta}_6^A \end{bmatrix} = \begin{bmatrix} I_{3 \times 3} & 0 \\ S_{(1;3,:)} \end{bmatrix} \begin{bmatrix} \dot{\theta}_a^A \\ \dot{\theta}_p^A \end{bmatrix}, \text{ and } \begin{bmatrix} \dot{\theta}_1^B \\ \vdots \\ \dot{\theta}_6^B \end{bmatrix} = \begin{bmatrix} 0 & I_{3 \times 3} \\ S_{(4;5,:)} \end{bmatrix} \begin{bmatrix} \dot{\theta}_a^A \\ \dot{\theta}_p^A \end{bmatrix} \quad (19)$$

where  $S_{(1;3,:)}$  is the first 3 rows of matrix  $S$  and  $S_{(4;5,:)}$  is the 4<sup>th</sup> and 5<sup>th</sup> row of  $S$ . From Eq. (19), we can now express the entire  $\dot{\theta}$  as the function of the active joint rates  $\dot{\theta}_a$  as:

$$\begin{bmatrix} \dot{\theta}_1^A \\ \vdots \\ \dot{\theta}_6^A \\ \vdots \\ \dot{\theta}_1^B \\ \vdots \\ \dot{\theta}_5^B \end{bmatrix}_{11 \times 1} = \begin{bmatrix} I_{3 \times 3} & 0_{3 \times 3} \\ S_{(1:3,:)} & - \\ 0_{3 \times 3} & I_{3 \times 3} \\ S_{(4:5,:)} & \end{bmatrix}_{11 \times 6} \begin{bmatrix} \dot{\theta}_1^A \\ \dot{\theta}_2^A \\ \dot{\theta}_3^A \\ \dot{\theta}_1^B \\ \dot{\theta}_2^B \\ \dot{\theta}_3^B \end{bmatrix}_{11 \times 6} \quad (20)$$

The Jacobian relating the end effector angular and linear velocities to the actuated joint rates can be written as:

$$\begin{bmatrix} \omega \\ v \end{bmatrix} = \underbrace{J^A \begin{bmatrix} I_{3 \times 3} & 0 \\ S_{(1:3,:)} & - \end{bmatrix}}_{J_T} \begin{bmatrix} \dot{\theta}_a^A \\ \dot{\theta}_a^B \end{bmatrix} = J_T \begin{bmatrix} \dot{\theta}_a^A \\ \dot{\theta}_a^B \end{bmatrix} \quad (21)$$

Alternately, we can partition Eq. (21) to the linear velocity and the angular velocity as follow:

$$\begin{aligned} \omega &= J_\omega \dot{\theta}_a \\ v &= J_v \dot{\theta}_a \end{aligned} \quad (22)$$

where  $J_\omega = J_{T(1:3,:)}$  and  $J_v = J_{T(4:5,:)}$ . Performing all these operations symbolically using Maple allows development of closed form expression for all elements of  $J_T$ . Three types of singularities can occur when either of  $J_A$ , or  $J_p$ , or  $J_p^{-1}J_A$  loses rank, all of which are easily detectable by virtue of the symbolic formulation.

## 5 VIRTUAL-PROTOTYPE/HARDWARE-IN-THE-LOOP TEST RIG

We examined design, analysis, prototyping, controller design and ultimately validation using a combination of virtual prototyping and hardware-in-the-loop testing. Our paradigm for rapid development, refinement and implementation of system design emphasizes: (i) development of the control scheme in a user-friendly, graphical, high-level block diagrammatic language (using MATLAB/Simulink) (ii) simulation, testing and refinement of the control system by virtual prototyping (using COTS simulation tools); (iii) rapid conversion of the refined control system into a form suitable for real-time execution (using Real-Time-Workshop/QuARC) for hardware-in-the-loop testing, as shown in Figure 4.

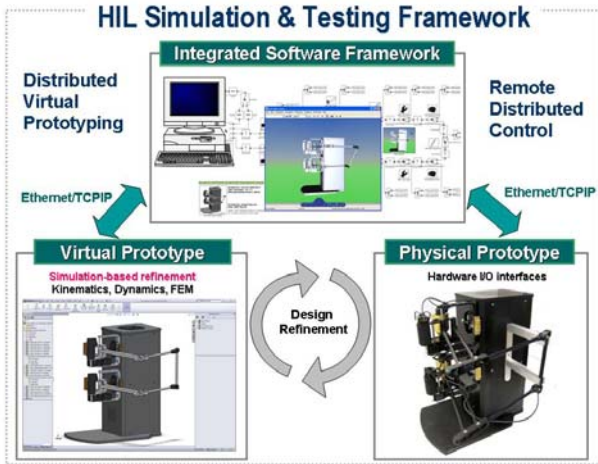


Figure 4. Hardware-In-the-Loop Design and Testing.

## 5.1 Trajectory Tracking

We seek to verify the ability to simulate the system together with a trajectory following task. A task-space controller was developed to allow the end-effector tip (position only) to track a moving spatial trajectory describe as  $x^d = R \sin(t)$ ;  $y^d = R \cos(t)$ ; and  $z^d = \cos(2t)$ , as  $t = 0 \rightarrow 2\pi$ . There is no requirement on the end-effector angles. The controller takes the following form:

$$\dot{\theta} = [J_v]^{-1} (\dot{x}^d + K(x^d - x)) \quad (23)$$

and an initial offset position of the end-effector (where frame  $\{7\}$  locate) by 0.25 in the  $z$  direction of frame  $\{0\}$ . In Figure 5, the desired trajectory and the actual trajectory of the end-effector is plotted. We see the convergence of the error and track the desired trajectory well. Figure 6 shows the angle profile of all the joints during the trajectory tracking and Figure 7 shows the trajectory tracking of the  $HD^2$  in the inertial frame.

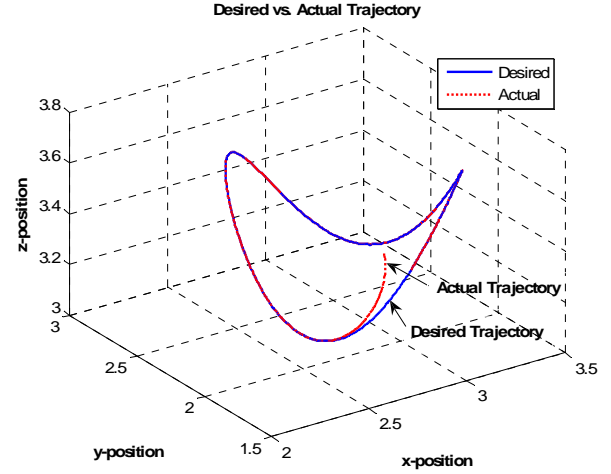


Figure 5. Trajectory tracking shows the end-effector of the  $(HD)^2$  track the given trajectory closely.

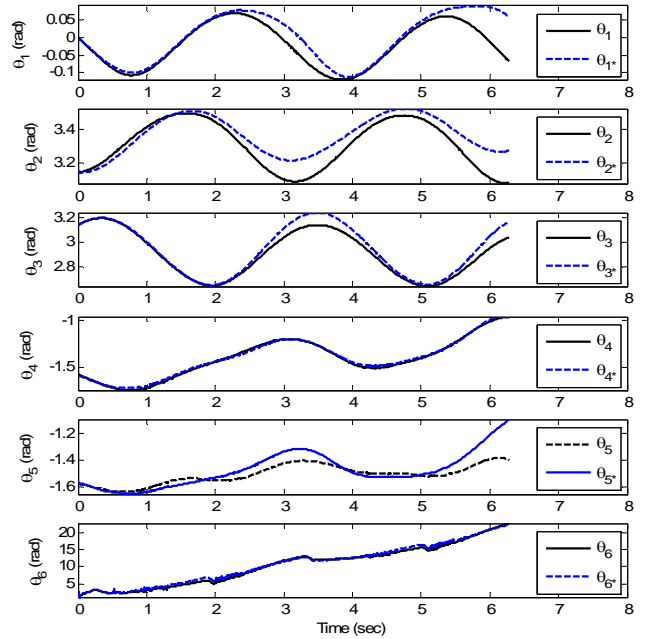


Figure 6. Angle profile of all the joints during the trajectory tracking.

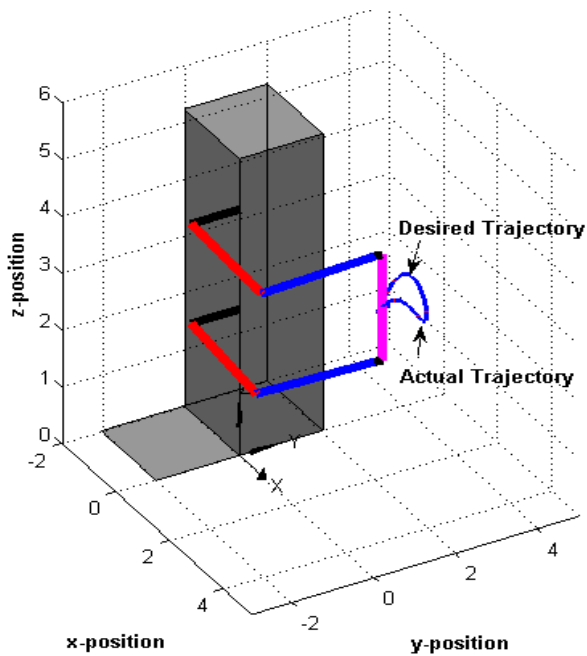


Figure 7. The trajectory tracking task performed by the HD<sup>2</sup>.

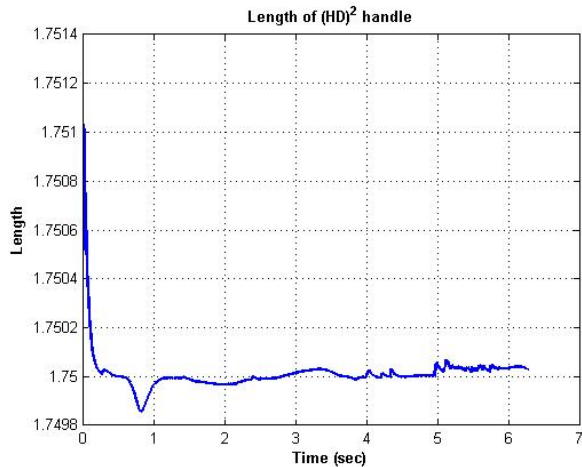


Figure 8. Length of the handle throughout the simulation showing constraints error is within  $1 \times 10^{-3}$ .

Currently efforts are also underway to use the symbolic equations to help identify singularities, design, and help improve real-time model based control strategies.

## 6 CONCLUSION

Modularly piecing together several serial-chain haptic-devices to form an in-parallel haptic device can potentially enhance overall capacity, robustness, reliability and reconfigurability. However, this enhanced capability needs to be realized by careful design and coordinated control (at both of the individual arm-levels as well as the system-level). The twist-based framework for performance-analysis and control-development permitted a systematic means to obtain both the individual-arm Jacobians as well as for the in-parallel system Jacobian. We illustrated these issues in the context of design and control of a novel in-parallel haptic device – the Quanser High Definition Haptic Device HD<sup>2</sup>. Our emphasis herein was on developing systematic and

algorithmic approaches and especially exploiting symbolic computational tools. The resulting symbolic equations facilitate insight into the structure as well as efficient means combined symbolic/numeric analyses of performance (such as workspace, singularities, for design refinement). Currently our efforts focused on the use of the symbolic equations to help identify singularities, perform parametric design refinements and help improve real-time model based control strategies.

## REFERENCES

- [1] K. W. Lilly, *Efficient Dynamic Simulation of Robotic Mechanisms*, 1 ed.: Springer, 1993.
- [2] S. McMillan, "Computational Dynamics for Robotic Systems on Land and Under Water," Ph.D., The Ohio State University, Columbus, Ohio, 1994.
- [3] L. Birglen, *et al.*, "SHaDe, a new 3-dof haptic device," *IEEE Transactions on Robotics and Automation*, vol. 18, pp. 166-175, 2002.
- [4] C. L. Collins and L. G. L., "The singularity analysis of an in-parallel hand controller for force-reflected teleoperation," *IEEE Transactions on Robotics and Automation*, vol. 11, pp. 661-669, 1995.
- [5] S. K. Agrawal and B. Roth, "Statics of in-parallel manipulators," *Journal of Mechanical Design, Transactions of the ASME*, vol. 114, pp. 564-568, 1992.
- [6] M. Y. Lee, *et al.*, "Development of kinematic/kinetic performance tools in the synthesis of multi-degree-of-freedom mechanisms," *ASME Journal of Mechanical Design*, vol. 115, pp. 392-402, 1993.
- [7] K. van den Doel and D. K. Pai, "Performance measures for robot manipulators: A unified approach," *The International Journal of Robotics Research*, vol. 15, pp. 92-111, 1996.
- [8] S. H. Murphy, *et al.*, "Simulation of cooperating robot manipulators on a mobile platform," *IEEE Transactions on Robotics and Automation*, vol. 7, pp. 468-478, 1991.
- [9] G. Rodriguez, "Recursive forward dynamics for multiple robot arms moving a common task object," *IEEE Transactions on Robotics and Automation*, vol. 5, pp. 510-521, 1989.
- [10] E. Paljug, *et al.*, "Control of rolling contacts in multi-arm manipulation," *IEEE Transactions on Robotics and Automation*, vol. 10, pp. 441-452, 1994.
- [11] X. Yun and V. Kumar, "An approach to simultaneous control of trajectory and interaction forces in dual arm configurations," *IEEE Transactions on Robotics and Automation*, vol. 7, pp. 97-109, 1991.
- [12] Y. Zheng and J. Y. S. Luh, "Optimal load distribution for two industrial robots handling a single object," in *IEEE International Conference on Robotics and Automation*, Philadelphia, PA, 1988, pp. 344-349.
- [13] H. Cheng, *et al.*, "Dynamics and control of redundantly actuated parallel manipulators," *IEEE/ASME Transactions on Mechatronics*, vol. 8, pp. 483-491, 2003.
- [14] T. Geike and J. McPhee, "Inverse dynamics analysis of parallel manipulators with full mobility," *Mechanism and Machine Theory*, vol. 38, pp. 549-562, 2003.
- [15] J. Kövecses, *et al.*, "Dynamics modeling and simulation of constrained robotic systems," *IEEE/ASME Transactions on Mechatronics*, vol. 8, pp. 165-177, 2003.
- [16] V. Kumar and K. J. Waldron, "Force distribution in closed kinematic chains," *IEEE Transactions on Robotics and Automation*, vol. 4, pp. 657-664, 1988.
- [17] K. H. Hunt, *Kinematic Geometry of Mechanisms*. Oxford: Clarendon Press, 1978.